29 June 2000

Dynamics of Glueball and $q\bar{q}$ production in the central region of pp collisions

Frank E. Close[1]

CERN, Geneva, Switzerland

and

Rutherford Appleton Laboratory

Chilton, Didcot, OX11 0QX, England

Andrew Kirk[2]

School of Physics and Space Research

Birmingham University

Gerhard Schuler[3]

CERN, Geneva, Switzerland

Abstract

We explain the ϕ and t dependences of mesons with $J^{PC} = 0^{\pm+}, 1^{++}, 2^{\pm+}$ produced in the central region of pp collisions. For the 0^{++} and 2^{++} sector this reveals a systematic behaviour in the data that appears to distinguish between $q\bar{q}$ and non-$q\bar{q}$ or glueball candidates.

[1]e-mail: F.E.Close@rl.ac.uk

[2]e-mail: ak@hep.ph.bham.ac.uk

[3]e-mail: Gerhard.Schuler@cern.ch

The idea that glueball production might be favoured in the central region of $pp \to pMp$ by the fusion of two Pomerons ($I\!P$) is over twenty years old [1, 2]. The fact that known $q\bar{q}$ states also are seen in this process frustrated initial hopes that such experiments would prove to be a clean glueball source. However, in [3] we noted a kinematic effect whereby known $q\bar{q}$ states could be suppressed leaving potential glueball candidates more prominent. There has been an intensive experimental programme in the last two years by the WA102 collaboration at CERN, which has produced a large and detailed set of data on both the dP_T [3] and the azimuthal angle, ϕ, dependence of meson production[1].

The azimuthal dependences as a function of J^{PC} and the momentum transferred at the proton vertices , t, are very striking. As seen in refs. [4, 5], and later in this paper, the ϕ distributions for mesons with $J^{PC} = 0^{-+}$ maximise around 90^o, 1^{++} at 180^o and 2^{-+} at 0^o. Recently, the WA102 collaboration has confirmed that this is not simply a J-dependent effect [6] since 0^{++} production peaks at 0^o for some states whereas others are more evenly spread [7]; 2^{++} established $q\bar{q}$ states peak at 180^o whereas the $f_2(1950)$, whose mass may be consistent with the tensor glueball predicted in lattice QCD, peaks at 0^o [6].

In this paper we show how these phenomena arise and in turn expose the extent to which they could be driven, at least in part, by the internal structure of the meson in question and thereby be exploited as a glueball/$q\bar{q}$ filter [3]. We find that the ϕ dependences of 0^{-+} and 1^{++} follow on rather general grounds if a single trajectory dominates the production mechanism. Having thus established the ability to describe the phenomena quantitatively in these cases, we predict the behaviour for 2^{-+} production and then confront the 0^{++} and 2^{++} *glueball*/$q\bar{q}$ sector.

$J^{PC} = 0^{-+}$

Parity forbids the production of 0^{-+} by the fusion of two scalars and also by the longitudinal ("L") components of two vectors. Transverse ("T") components are allowed and so we focus on the TT component of $I\!P$- $I\!P$ fusion in the production of the 0^{-+} states. $\rho\rho$ fusion is also possible, however, in this paper we will concentrate on the η' meson whose production has been found to be consistent with double pomeron exchange [4].

The calculations have been described in [8, 9] and the resulting behaviour of the cross section may be summarised as follows:

$$\frac{d\sigma}{dt_1 dt_2 d\phi'} \sim t_1 t_2 G_E^{p\,2}(t_1) G_E^{p\,2}(t_2) \sin^2(\phi') F^2(t_1, t_2, M^2)$$

[1] dP_T is the difference in the transverse momentum vectors of the two exchange Pomerons and ϕ is the angle between the transverse momentum vectors, p_T, of the two outgoing protons.

where ϕ' is the angle between the two pp scattering planes in the $I\!P$- $I\!P$ centre of mass and $F(t_1, t_2, M^2)$ is the $I\!P$- $I\!P$-η' form factor. We temporarily set this equal to unity; pp elastic scattering data and/or a Donnachie Landshoff type form factor [10] can be used as model of the proton- $I\!P$ form factor ($G_E^p(t)$). This ϕ' distribution is shown in fig. (1a) and applies in the meson rest frame (current-current c.m.) in the "symmetric" configuration, $t_1 = t_2; \vec{p}_{T1} = -\vec{p}_{T2}; x_F = 0$. To generalise to real kinematics, we use a Monte Carlo simulation based on Galuga [11] modified for pp interactions and incorporating the $I\!P$-proton form factor from ref. [10]. This has the effect of distorting fig. (1a) to fig. (1b).

The WA102 collaboration measures the azimuthal angle (ϕ) in the pp c.m. frame and so we transform the ϕ' from the current c.m. frame to ϕ for the pp c.m. frame. For the 0^{-+} case it happens that the above two steps (fig. (1a) to fig. (1b) and this) tend to counterbalance. Using the modified form of the Galuga Monte Carlo, discussed above, we can now compare these predictions with the experimental data, taking into account the experimental cuts and the geometrical acceptance corrections of the WA102 experiment. Any differences between the output of the Monte Carlo model predictions and the data are then due to intrinsic physics and not to experimental acceptance effects.

In order to fit the data we found that the $I\!P$- $I\!P$-meson form factor $F(t_1, t_2, M^2)$ has to differ from unity. If we parametrise $F^2(t_1, t_2, M^2)$ as $exp^{-b_T(t_1+t_2)}$ then we need $b_T = 0.5\ GeV^{-2}$ in order to describe the t dependence. Fig. (1c and 1d) compare the final theoretical form for the ϕ distribution and the t dependence with the data for the η'. The distributions are well described also for the η but it has not yet been established that $I\!P$- $I\!P$ alone dominates the production of this meson.

$J^{PC} = 1^{++}$

In refs. [8, 9, 12] Close and Schuler have predicted that axial mesons are produced polarised, dominantly in helicity one; this is verified by data [13]. The cross section is predicted to have the form

$$\frac{d\sigma}{dt_1 dt_2 d\phi'} \sim t_1 t_2 [\{A(t_1^T, t_2^L) - A(t_2^T, t_1^L)\}^2 + 4A(t_1^T, t_2^L)A(t_1^L, t_2^T)\sin^2(\phi'/2)]$$

where $A(t_i, t_j)$ are the $I\!P$- $I\!P$-f_1 form factors. In the models of refs. [9, 14] the longitudinal Pomeron amplitudes carry a factor of $1/\sqrt{t}$ arising from the fact that, in the absence of any current conservation for the Pomeron, a longitudinal vector polarisation is not compensated. Thus we make this factor explicit and write $A(t_i, t_j^L) = \frac{\mu}{\sqrt{t_j}} a(t_i, t_j)$. The cross section is predicted to behave as

$$\frac{d\sigma}{dt_1 dt_2 d\phi'} \sim [\{\sqrt{t_1} - \sqrt{t_2}\frac{a(t_1^T, t_2^L)}{a(t_1^L, t_2^T)}\}^2 + 4\sqrt{t_1 t_2}\frac{a(t_1^T, t_2^L)}{a(t_1^L, t_2^T)}\sin^2(\phi'/2)]a^2(t_1^L, t_2^T)$$

In the particular case where the ratio of form factors is unity, this recovers the form used in ref. [9]

$$\frac{d\sigma}{dt_1 dt_2 d\phi'} \sim [(\sqrt{t_1} - \sqrt{t_2})^2 + 4\sqrt{t_1 t_2}\sin^2(\phi'/2)]a^2(t_1, t_2)$$

which implies a dominant $\sin^2(\phi/2)$ behaviour that tends to isotropy when suitable cuts on t_i are made. This is qualitatively realised (figs. 1e and f of ref. [4]).

We have parametrised $a(t_i^T, t_j^L)$ as an exponential, $exp^{-(b_T t_i + b_L t_j))}$ where $i, j = 1, 2$; $b_T = 0.5$ GeV^{-2} was determined from the η' data above; b_L is determined from the overall t dependence of the 1^{++} production and requires $b_L = 3$ GeV^{-2}. Fig. (2a and b) show the output of the model predictions from the Galuga Monte Carlo superimposed on the ϕ and t distributions for the $f_1(1285)$ from the WA102 experiment.

In addition we have a parameter free prediction of the variation of the ϕ distribution as a function of $|t_1 - t_2|$. Fig. (2c and d) show the output of the Galuga Monte Carlo superimposed on the ϕ for the $f_1(1285)$ for $|t_1 - t_2| \leq 0.2$ GeV^{-2} and $|t_1 - t_2| \geq 0.4$ GeV^{-2} respectively. The agreement between the data and our prediction is excellent. Similar conclusions arise for the $f_1(1420)$.

$J^{PC} = 2^{-+}$

The $J^{PC} = 2^{-+}$ states, the $\eta_2(1645)$ and $\eta_2(1870)$, are predicted to be produced polarised. Helicity 2 is suppressed by Bose symmetry [8] and has been found to be negligible experimentally [5]. The structure of the cross section is then predicted to be

(i) helicity zero: as for the 0^{-+} case,

$$\frac{d\sigma}{dt_1 dt_2 d\phi'} \sim t_1 t_2 \sin^2(\phi')$$

(ii) helicity one:

$$\frac{d\sigma}{dt_1 dt_2 d\phi'} \sim [\{\sqrt{t_1} - \sqrt{t_2}\frac{a(t_1^T, t_2^L)}{a(t_1^L, t_2^T)}\}^2 + 4\sqrt{t_1 t_2}\frac{a(t_1^T, t_2^L)}{a(t_1^L, t_2^T)}\cos^2(\phi'/2)]a^2(t_1^L, t_2^T)$$

which is as the 1^{++} case except for the important and significant change from $\sin^2(\phi'/2)$ to $\cos^2(\phi'/2)$.

The intrinsic relative strengths of the two helicity amplitudes will depend upon the internal dynamics of the $I\!P$- $I\!P$-η_2 vertex which are beyond the scope of the present paper. The uncompensated factor of $t_1 t_2$ in the helicity zero component will tend to suppress this kinematically under the conditions of the WA102 experiment. Indeed, WA102 find that helicity one alone is able to describe their data [5]; this is in interesting contrast to $\gamma\gamma \to \eta_2(Q\bar{Q})$ in the non-relativistic quark model where the helicity-one amplitude would be predicted to vanish [15]. We shall concentrate on this helicity-one amplitude henceforth.

The results of the WA102 collaboration for the $\eta_2(1645)$ [5] are shown in fig. (3a and b). The distribution peaks as $\phi \to 0$, in marked contrast to the suppression in the 1^{++} case (fig. 2a).

Integrating our formula over ϕ, with the same approximations as previously, implies

$$\frac{d\sigma}{dt_1 dt_2} \sim (t_1 + t_2)(exp^{-(b(t_1+t_2)})$$

and, in turn, that

$$\frac{d\sigma}{dt} \sim (1 + bt)(exp^{-bt}) \tag{1}$$

This simple form compares remarkably well with WA102 who fit to $\alpha e^{-b_1 t} + \beta t e^{-b_2 t}$; our prediction (eq. 1) implies that $b_1 \equiv b_2$ and that $\beta/\alpha \equiv b$ and WA102 find for the $\eta_2(1645)$) [5] $b_1 = 6.4 \pm 2.0; b_2 = 7.3 \pm 1.3$ and $\beta = 2.6 \pm 0.9$, $\alpha = 0.4 \pm 0.1$

Performing the detailed comparison of model and data via Galuga, as in the previous examples, leads to the results shown in fig. (3a and b) for the $\eta_2(1645)$; the $\eta_2(1870)$ results are qualitatively similar. Bearing in mind that there are no free parameters, the agreement is remarkable. Indeed, the successful description of the 0^{-+}, 1^{++} and 2^{-+} sectors, both qualitatively and in detail, set the scene for our analysis of the 0^{++} and 2^{++} sectors where glueballs are predicted to be present together with established $q\bar{q}$ states. Any differences between data and this model may then be a signal for hadron structure, and potentially a filter for glue degrees of freedom.

$J^{PC} = 0^{++}$ and 2^{++}

In contrast to the 0^{-+} case, where parity forbade the LL amplitude, in the 0^{++} case both TT and LL can occur. Hence there are two independent form factors [16] $A_{TT}(t_1, t_2, M^2)$ and $A_{LL}(t_1, t_2, M^2)$. For 0^{++} and the helicity zero amplitude of 2^{++} (which experimentally is found to dominate [17]) the angular dependence of scalar meson production will be [9]

$$\frac{d\sigma}{dt_1 dt_2 d\phi'} \sim {G_E^p}^2(t_1){G_E^p}^2(t_2)[1 + \frac{\sqrt{t_1 t_2}}{\mu^2}\frac{a_T}{a_L}e^{(b_L - b_T)(t_1+t_2)/2}\cos(\phi')]^2 e^{-b_L(t_1+t_2)} \qquad (2)$$

where we have written $a_L(t) = a_L e^{-(b_L t/2)}$ and $a_T(t) = a_T e^{-(b_T t/2)}$ with $b_{L,T}$ fixed to the values found earlier. The ratio a_T/a_L can be positive or negative, or in general even complex.

Eq.(2) predicts that there should be significant changes in the ϕ distributions as t varies. When $\frac{\sqrt{t_1 t_2}}{\mu^2} a_T/a_L \sim \pm 1$, the ϕ distribution will be $\sim \cos^4(\frac{\phi}{2})$ or $\sin^4(\frac{\phi}{2})$ depending on the sign. Indeed data on the enigmatic scalars $f_0(980)$ and $f_0(1500)$ show a $\cos^4(\frac{\phi}{2})$ behaviour when $\sqrt{t_1 t_2} \leq 0.1$ GeV^2, changing to $\sim \cos^2(\phi)$ when $\sqrt{t_1 t_2} \geq 0.3$ GeV^2 [4].

In this paper we show how the overall ϕ dependences for the $f_0(1370)$, $f_0(1500)$, $f_2(1270)$ and $f_2(1950)$ can be described by varying the quantity $\mu^2 a_L/a_T$. Results are shown in fig. 4. It is clear that these ϕ dependences discriminate two classes of meson in the 0^{++} sector and also in the 2^{++}. The $f_0(1370)$ can be described using $\mu^2 a_L/a_T$ = -0.5 GeV^2, for the $f_0(1500)$ it is +0.7 GeV^2, for the $f_2(1270)$ it is -0.4 GeV^2 and for the $f_2(1950)$ it is +0.7 GeV^2.

It is interesting to note that we can fit these ϕ distributions with one parameter and it is primarily the sign of this quantity that drives the ϕ dependences. Understanding the dynamical origin of this sign is now a central issue in the quest to distinguish $q\overline{q}$ states from glueball or other exotic states.

In summary, for the production of $J^{PC} = 0^{-+}$ mesons we can predict the ϕ dependence and the vanishing cross section as $t \to 0$ absolutely and fit the t slope in terms of one parameter, b_T. For the $J^{PC} = 1^{++}$ mesons we predict the general form for the ϕ distribution. By fitting the t slope we obtain the parameter b_L; this then gives a parameter free prediction for the variation of the ϕ distribution as a function of t which agrees with the data. In addition, these give absolute predictions for the t and ϕ dependences of the $J^{PC} = 2^{-+}$ mesons which are again in accord with the data when helicity 1 dominance is imposed. For the 0^{++} and 2^{++} sector we extract a systematic behaviour from the data that requires a dynamical interpretation. Whether this is the long sought discriminator between $q\bar{q}$ and non-$q\bar{q}$ states is for the future.

Acknowledgements

This work is supported, in part, by grants from the British Particle Physics and Astronomy Research Council, the British Royal Society, the European Community Human Mobility Program Eurodafne, contract NCT98-0169 and the EU Fourth Framework Programme contract FMRX-CT98-0194.

References

[1] D. Robson, Nucl. Phys. **B130** (1977) 328.

[2] F.E. Close, Rep. Prog. Phys. **51** (1988) 833.

[3] F.E. Close and A. Kirk, Phys. Lett. **B397** (1997) 333.

[4] D. Barberis *et al.,* Phys. Lett. **B467** (1999) 165.

[5] D. Barberis *et al.,* hep-ex/9911038 To be published in Phys. Lett.

[6] D. Barberis *et al.,* arXiv:hep-ex/0001017 To be published in Phys. Lett.

[7] D. Barberis *et al.,* Phys. Lett. **B462** (1999) 462.

[8] F.E. Close and G.A. Schuler, Phys. Lett. B458 (1999) 127.

[9] F.E. Close and G.A. Schuler, Phys. Lett. B464 (1999) 279.

[10] A. Donnachie and P.V. Landshoff, Nucl. Phys. **B231** (1983) 189.

[11] G.A. Schuler, Comput. Phys. Commun. **108** (1998) 279.

[12] F.E. Close, Phys. Lett. **B419** (1998) 387.

[13] D. Barberis *et al.,* Phys. Lett. **B440** (1998) 225.

[14] T. Arens, O. Nachtmann, M. Diehl and P.V. Landshoff, Z. Phys **C74** (1997) 651.

[15] F.E. Close and Zhenping Li, Z. Phys. **C54** (1992) 147.

[16] F.E. Close, G.Farrar and Z.P.Li, Phys. Rev. **D55** (1997) 5749.

[17] D. Barberis *et al.,* Phys. Lett. **B453** (1999) 305;
D. Barberis *et al.,* Phys. Lett. **B453** (1999) 316.

Figures

Figure 1: The predicted ϕ' distributions for $J^{PC} = 0^{-+}$ mesons a) naive distribution and b) taking into account the experimental kinematics. c) The ϕ and d) the $|t|$ distributions for the η' for the data (dots) and the model predictions from the Monte Carlo (histogram).

Figure 2: a) The ϕ and b) the $|t|$ distributions for the $f_1(1285)$ for the data (dots) and the Monte Carlo (histogram). c) and d) the ϕ distributions for $|t_1 - t_2| \leq 0.2$ and $|t_1 - t_2| \geq 0.4\ GeV^2$ respectively.

Figure 3: a) The ϕ and b) the $|t|$ distributions for the $\eta_2(1645)$ for the data (dots) and the Monte Carlo (histogram).

Figure 4: The ϕ distributions for the a) $f_0(1370)$, b) $f_0(1500)$, c) $f_2(1270)$ and d) $f_2(1950)$ for the data (dots) and the Monte Carlo (histogram).

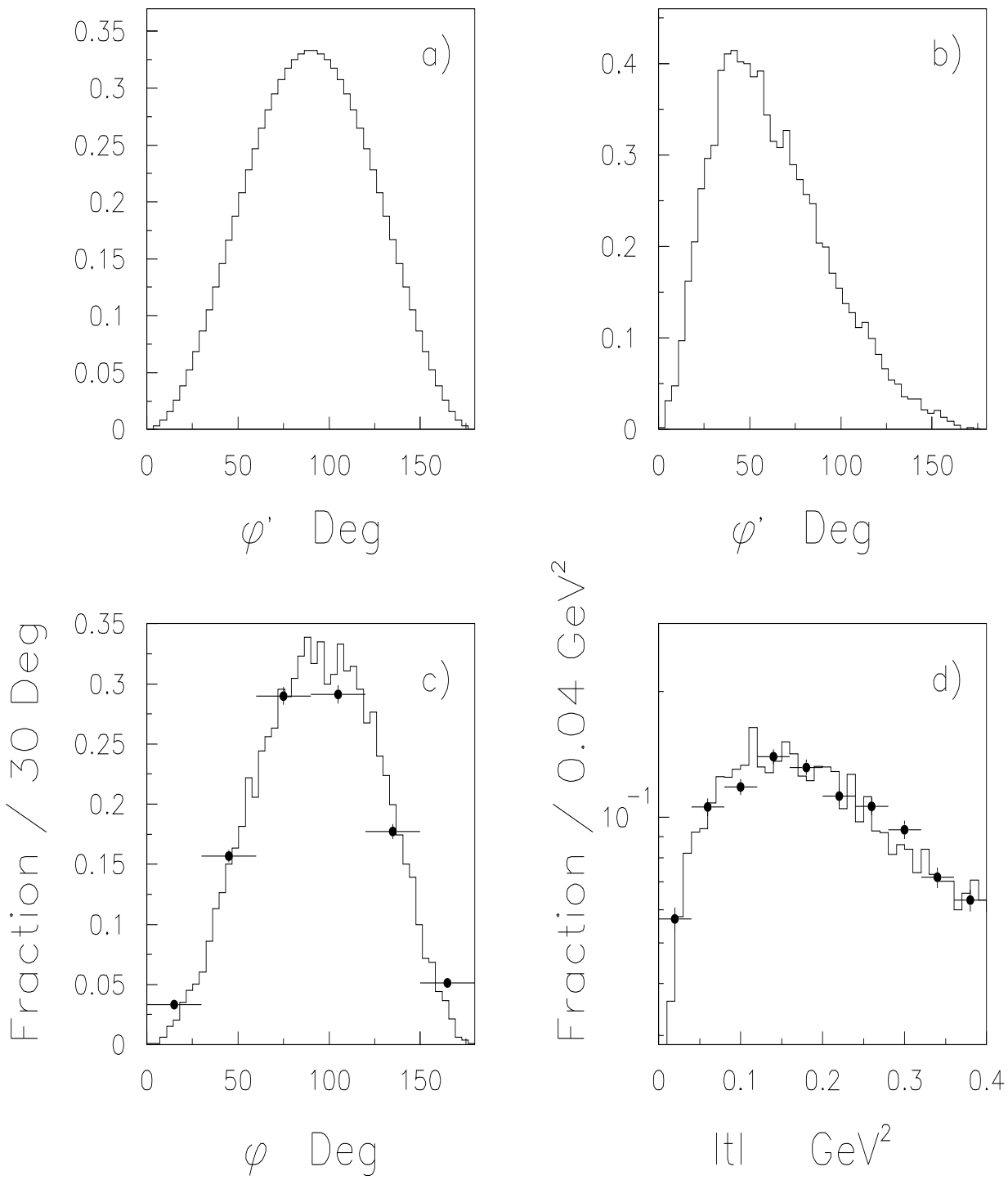
a)
b)
c)
d)
0.35
0.3
0.25
0.2
0.15
0.1
0.05
0
0.4
50
100
150
φ' Deg
φ Deg
Fraction / 30 Deg
Fraction / 0.04 GeV²
10⁻¹
0.1
0.2
0.3
0.4
|t| GeV²

Figure 1

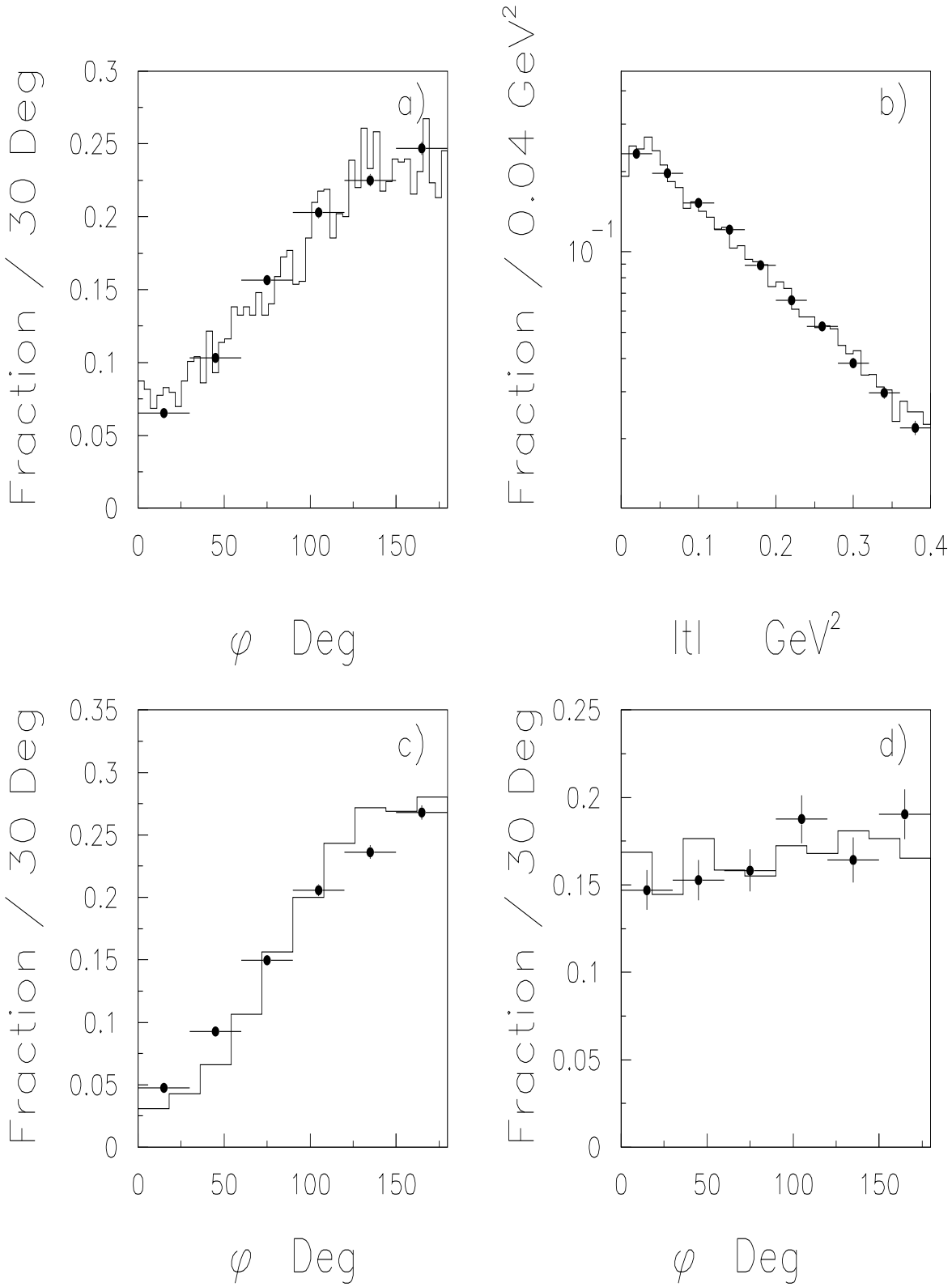
a)
b)
c)
d)
Fraction / 30 Deg
Fraction / 0.04 GeV^2
10^{-1}
φ Deg
|t| GeV^2
0
0.05
0.1
0.15
0.2
0.25
0.3
0.35
0.4
50
100
150

Figure 2

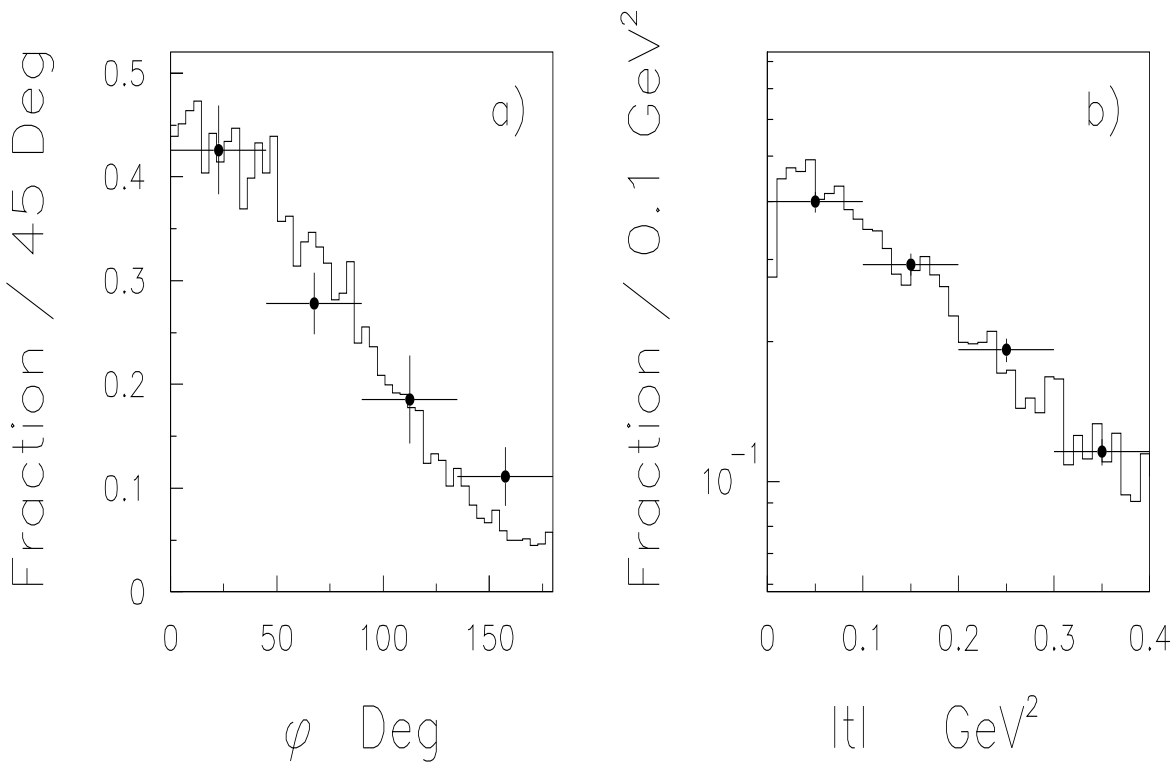
Fraction / 45 Deg
0.5
0.4
0.3
0.2
0.1
0
a)
0
50
100
150
φ Deg
Fraction / 0.1 GeV²
10⁻¹
b)
0
0.1
0.2
0.3
0.4
|t| GeV²

Figure 3

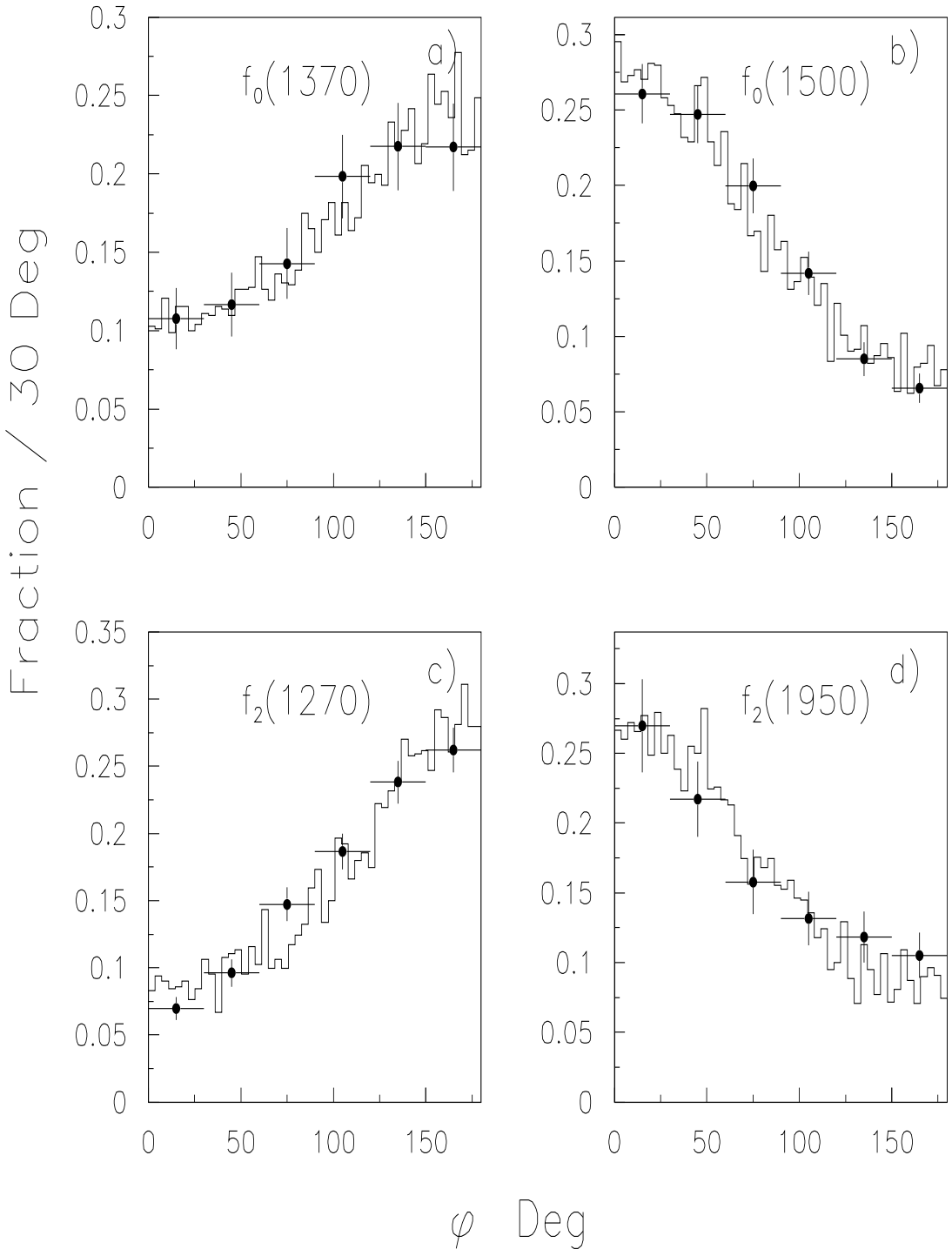
a)
$f_0(1370)$
b)
$f_0(1500)$
c)
$f_2(1270)$
d)
$f_2(1950)$
Fraction / 30 Deg
φ Deg

Figure 4